

Characteristics of Horizontal Winds in the Mesosphere and Lower Thermosphere Region over Korean Peninsula Observed from the Korea Astronomy and Space Science Institute Meteor Radar

Hosik Kam¹, Young-Sil Kwak^{1,2†}, Tae-Yong Yang¹, Yong Ha Kim³, Jeongheon Kim¹, Jaewook Lee^{1,2}, Seonghwan Choi¹, Ji-Hye Baek¹

¹Division of Space Science, Korea Astronomy and Space Science Institute, Daejeon 34055, Korea

²Korea University of Science and Technology, Daejeon 34113, Korea

³Department of Astronomy, Space Science and Geology, Chungnam National University, Daejeon 34134, Korea

We present for the first time the characteristics of upper atmospheric horizontal winds over the Korean Peninsula. Winds and their variability are derived using four-year measurements by the Korea Astronomy and Space Science Institute (KASI) meteor radar. A general characteristic of zonal and meridional winds is that they exhibit distinct diurnal and seasonal variations. Their changes indicate sometimes similar or sometimes different periodicities. Both winds are characterized by either semi-diurnal tides (12 hour period) and/or diurnal tides (24 hour period) from 80–100 km. In terms of annual change, the annual variation is the strongest component in both winds, but semi-annual and ter-annual variations are only detected in zonal winds.

Keywords: meteor radar, mesospheric winds, diurnal variation, annual variation

1. INTRODUCTION

The neutral horizontal winds in the mesosphere and lower thermosphere (MLT) region are related to the temperature through the balance of atmospheric thermal motion. Moreover, the dynamics in this region are controlled and varied by atmospheric waves of which periods are ranged from a few minutes to annual time scales. Especially, gravity waves whose periods are under a few hours, are originated from the lower atmosphere with upward propagation and are dissipated or broken by the dynamical or thermal instabilities in the upper atmosphere. The dissipated or broken waves play a role of changing the background flow and thermal structure in the upper atmosphere by the upward transportation of energy and momentum from the lower atmosphere to the background flow and thermal structure in the upper atmosphere. Their effects in the polar MLT region create a drag on the zonal wind and then drives a summer-to-winter

pole circulation by Coriolis force. This global meridional circulation causes vertical motions with adiabatically cooling (heating) the summer (winter) polar mesopause far away from the state of radiative balance (Holton & Wehrbein 1980; Lindzen 1981). Then, due to this circulation, the summer polar MLT region becomes the coldest region on Earth's atmosphere. In addition, semi-annual oscillation (SAO) in the tropical MLT region is known as a result of filtering effect, which allows the gravity wave as horizontally propagating opposite to the wind direction to do upward propagation and also modulate winds in a specific direction by wave forcing. Hence, the SAO phase of winds in the MLT region is out of phase with that of winds in the stratosphere (Garcia et al. 1997; Lieberman et al. 1997). Therefore, the dissipating or breaking gravity wave impacts background flow to drive sequential changes of the condition of global MLT region in various scales.

Atmospheric migrating tides are also regarded as one of the

© This is an Open Access article distributed under the terms of the Creative Commons Attribution Non-Commercial License (<https://creativecommons.org/licenses/by-nc/3.0/>) which permits unrestricted non-commercial use, distribution, and reproduction in any medium, provided the original work is properly cited.

Received 01 NOV 2021 Revised 30 NOV 2021 Accepted 03 DEC 2021

† Corresponding Author

Tel: +82-42-865-2039, E-mail: yskwak@kasi.re.kr

ORCID: <https://orcid.org/0000-0003-3375-8574>

most prominent atmospheric waves as a role of transporting energy and momentum from the lower to upper atmosphere. Migrating tides are global-scale dynamics in westward propagation following the solar apparent motion, having two dominant harmonics, including a diurnal (24-hour period) and a semi-diurnal (12-hour period). The diurnal tides can be generated by direct sunlight absorption of solar insolation for low atmospheric species such as water vapor (Lindzen & Chapman 1970), and the release of latent heat by water vapor is also an important source of diurnal tides in the lower atmospheres of tropical regions (Forbes & Vial 1989). In the meanwhile, the semi-diurnal tides are mainly generated by ozone absorption in the middle atmosphere such as the upper stratosphere and lower mesosphere. In addition, ter-diurnal (8-hour period) tides have been observed by both ground-based and satellite-based observations (Zhao et al. 2005; Pancheva et al. 2013), but their sources are uncertain due to relatively small amplitude compared to diurnal and semi-diurnal tides. One of the possible generating mechanisms is nonlinear interactions between other tides (Cevolani 1987; Thayaparan 1997). Observed amplitudes of short-term ter-diurnal tides are correlated with those of diurnal and semi-diurnal tides, and the vertical wavenumber is equal to the sum of those of diurnal and semi-diurnal tides according to Younger et al. (2002). Using a nonlinear mechanistic global circulation model, Lilienthal et al. (2018) analyzed removing a direct ter-diurnal solar heating leads to a significant decrease in their amplitude and then found possible mechanism as solar forcing directly. Based on observations at middle latitudes, the amplitude of ter-diurnal tide is turned out as the largest in winter (Thayaparan 1997; Smith 2000; Namboothiri et al. 2004).

In this regard, monitoring the horizontal winds in the MLT region is very important to understand the upper atmospheric environment, because horizontal winds in the MLT region at mid-latitude are important to understand the global circulation or mesospheric SAO and atmospheric waves can be measured and results regarding the impact of the atmospheric waves can be inferred. In this study, we analyze the horizontal winds (80–100 km) obtained from KASI (Korea Astronomy and Space Science Institute) meteor radar (MR) to investigate the characteristics of the upper atmosphere over Korean Peninsular.

2. OBSERVATION OF HORIZONTAL WINDS FROM METEOR RADAR

KASI MR has been operated at Daejeon (36.18°N, 124.14°E)

since October 2017 by KASI and is manufactured by ATRAD Pty. This instrument has two types of observing modes for detecting the ionospheric irregularities (Kwak et al. 2014; Yang et al. 2015; Yang et al. 2021) and meteor echo with a switching interval time of each 2 minutes. Exceptionally, from September 12, 2020 to September 24, 2020, KASI radar was operated only in MR mode without observing ionospheric irregularities. KASI MR is an interferometric radar consisting of a cross-folded dipole transmitting antenna and 5 receiving antennas arranged in two perpendicular directions having spacings of 2.5λ and 2.0λ to provide unambiguous directions to investigate the accuracy angle of arrival estimation (Holdsworth 2005), where λ is the wavelength of wave transmitted from MR. The radar configuration has a central frequency of 40.8 MHz, a pulse repetition of 440 Hz, and transmitting peak power of 24 kW. MR detects meteor echo by a perpendicular back-scattered signal from entrancing meteor induced plasma trail, and it provides us with spatial information of meteor echoes such as echo distance (range from radar), azimuth, and zenith angle estimated from phase comparison of pair for individual MR receive-antenna as a cross-dipole interferometry system.

The principle of horizontal wind measurement is to exploit the radial velocity of the echo detected in the Doppler shift of backscattered VHF waves in a meteor plasma trail. The radial velocity provides along the line of sight of the incident wave signal. When deriving a horizontal wind at a radial velocity, the normal vertical wind is 1–2 times smaller than the horizontal wind, so it is considered zero. To measure the horizontal winds from MR, the observed echoes are allocated into time-altitude bins with a minimum interval time of 1 hour and a vertical sampling resolution of 2 km from 80–100 km heights. Then, from the radial velocity, the horizontal wind velocity is estimated using the linear least-squares method. A fitting analysis of meteor echo requires 6 echoes and is performed when the difference between the observed radial velocity and the linearly fitted radial velocity is less than 25 m/s. The detailed method for estimating horizontal winds from MR is well described in Holdsworth et al. (2004). The available range of the zenith angle is from 15° to 75° to reduce an uncertainty of spatial information of meteor echo. Since the meteor echo detected in a relatively large zenith angle is subjected to significant atmospheric effects such as near-horizon reflections, water vapor, ions, and electrons in the path of the back-scattered signal, it is difficult to determine the correct spatial information. When echo is detected near the zenith direction, it is very difficult to measure the azimuthal information of echo and a significant estimation error can

occur when deriving the horizontal winds. In addition, in order to collect echoes with accurate spatial information, we use MR echoes with an average phase error of 6 or less. (Kam et al. 2019). In this study, we utilized the KASI MR horizontal winds from October 2017 to December 2020 about 4-year observation.

3. CHARACTERISTICS OF HOURLY HORIZONTAL WINDS

In order to estimate hourly horizontal winds, the time resolution for echo sampling is 1 hour with the vertical sampling resolution of 2 km in the altitude-time sector. Fig. 1 shows sample data of zonal wind (top) and meridional wind (bottom) observed from September 22nd, 2020 to September 28th, 2020 using KASI MR. In Fig. 1, the black dotted contour line indicates the wind speed is zero, and the color-coded contour lines indicate east-/northward winds in red for positive values and west-/southward winds in blue for negative values. Regions without wind values are grayed out and appear above $z = 95$ km and below $z = 85$ km at 3 UT (12 LT) – 12 UT (21 LT).

The absence of wind values occurs because the number of echo counts detected is too small to estimate the wind speed. Usually the magnitudes of horizontal wind are varied up to about 100 m/s, and their signs are changed within 24 hours at entire heights. It can be considered as the effect of atmospheric tides of horizontal winds. In other words, the vertical structure of the wind shows a downward phase, indicating that atmospheric tidal waves propagate upward over the Korean Peninsula. On September 28, between 0 UT and 12 UT, the descending structure in phase show a clear semi-diurnal tide with enhanced magnitude in both winds. However, most tidal structures are ambiguous to recognize periodic wind changes, especially in zonal winds. The reason why the vertical structure is unclear maybe that atmospheric gravity waves exert a force on the horizontal wind field in the MLT region and disturb it (Wu et al. 2013).

To investigate the tidal component, Fig. 2 shows Lomb-Scargle periodograms for hourly zonal (left) and meridional (right) winds for 4-year observations, with periodic components between $z = 80$ km and $z = 100$ km within a time period of 30 hours. Remarkably, strong periodic components for 12 and 24 hours are clearly detectable at

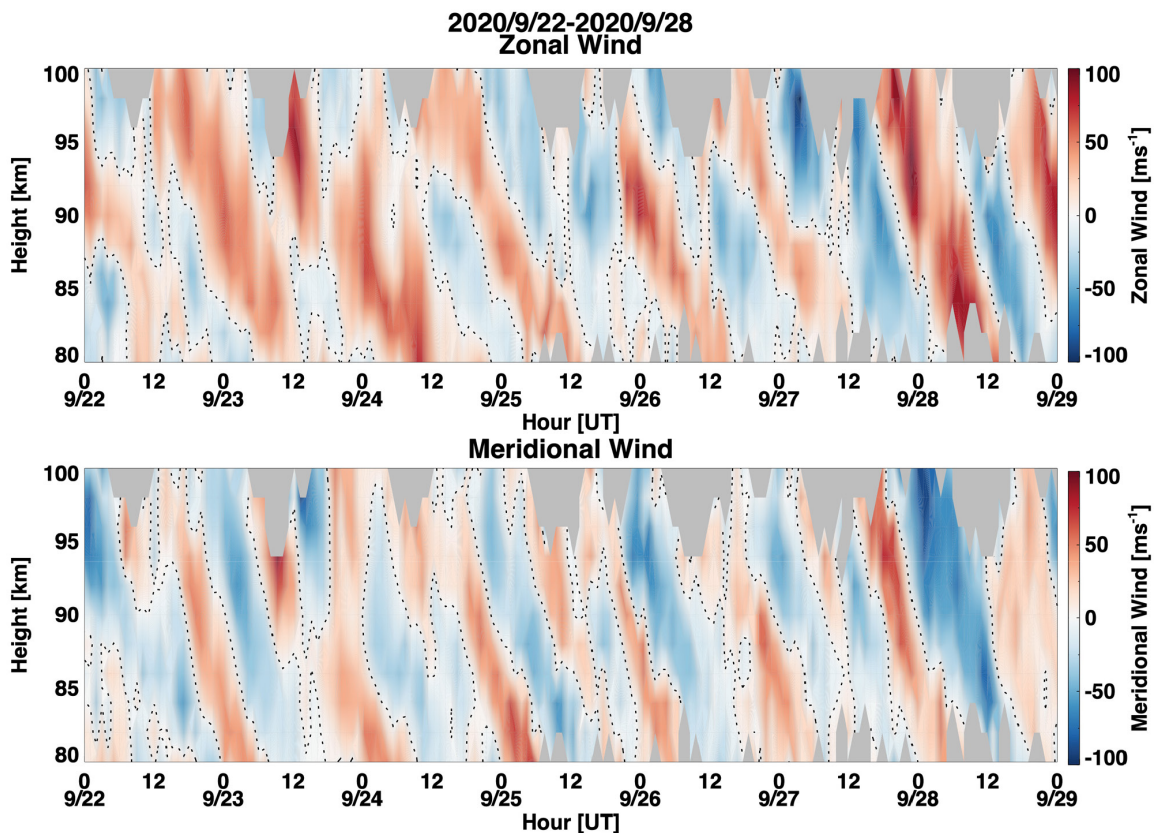


Fig. 1. Zonal (top) and meridional (bottom) winds in the MLT region over Korean Peninsula obtained from KASI MR for 1-week observation. MLT, mesosphere and lower thermosphere; KASI, Korea Astronomy and Space Science Institute.

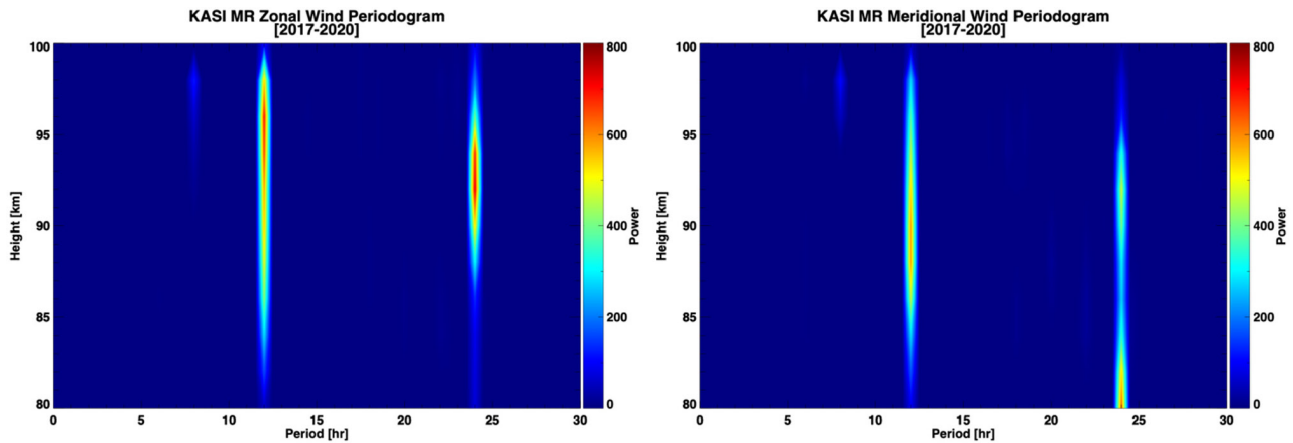


Fig. 2. Lomb-Scargle periodograms for hourly zonal (left) and meridional (right) winds in MLT region over Korean Peninsula obtained from KASI MR for 4-year observation. MLT, mesosphere and lower thermosphere; KASI, Korea Astronomy and Space Science Institute.

the zonal and meridional winds at the full height range (80–100 km). Therefore, we can infer that diurnal and semi-diurnal tidal waves are strongly present and may influence the dynamics of the MLT region of the Korean Peninsula. However, the maximum power for each of the tides varied according to height range. The magnitudes of the diurnal tide revealed a maximum height range of $z = 90\text{--}95$ km and $z = 80\text{--}83$ km in zonal and meridional winds, respectively. The altitude range of the strongest periodicity of the semi-diurnal tide in zonal winds is $z = 93\text{--}97$ km, while the altitude range of meridional winds is $z = 87\text{--}91$ km. It might imply that modulating or dissipating processes of diurnal and semi-diurnal tides in each direction are associated with different mechanisms such as the wave drag impact of filtered gravity waves, the effect of global meridional circulation, and so on. In Fig. 2, the relatively low power component of the 8-hour period, which appears only above $z = 95$ km in both periodograms, is considered a ter-diurnal tide. However, it could also be an artificial signal since the absence of data above $z = 95$ km (shown as the gray shaded area in Fig. 1). Meanwhile, further investigation of ter-diurnal tides will also be important to understand the dynamical characteristics in the MLT region over the Korean Peninsula.

4. CHARACTERISTICS OF DAILY HORIZONTAL WINDS

Like hourly horizontal winds, daily horizontal winds are measured from sampled meter echoes allocated into time-altitude bins with an interval time of 1 day and a vertical sampling resolution of 2 km from 80–100 km heights. The daily variation of winds is produced from the wind daily averaged, in which tidal effects are lost, and represent the characteristics of mean flow in the MLT region over Korean

Peninsula. As shown in Fig. 3, daily variations of horizontal winds reveal seasonal mean flow for zonal wind (left) and meridional wind (right) from $z = 80$ km to $z = 100$ km. The color-coded contours varying from blue to red indicate the same directions as given for Fig. 1, and thick line contours indicate zero speed of the mean wind. In zonal winds, westward jets occur below $z = 90$ km from April to July, and two eastward jets occur below $z = 85$ km in the time range from November to February and above $z = 90$ km from April to July. The patterns of zonal winds are fairly similar to the results of 8-year observations from Beijing (40.3°N , 116.2°E) MR (Tang et al. 2021). Moreover, westward wind fields near $z = 100$ km are detected at both Daejeon and Beijing. The similarities between the two sites of Daejeon and Beijing indicate that the jet stream is widely spread or connected east-west in the MLT region over the East Asian region. Usually, in summer westward wind fields in the stratosphere and mesosphere are determined by the atmospheric pressure gradients over latitudes caused by non-uniform solar radiation from the equator to the poles. The westward wind fields below $z = 90$ km can allow to propagate only eastward gravity waves, whereas westward gravity waves are blocked from propagating upward. Therefore, the penetrated eastward gravity waves above $z = 90$ km can transport eastward wave momentum on the horizontal wind in order to form eastward wind fields as seen in Fig. 3. The similar zonal wind fields are also shown for Beijing. In meridional winds below $z = 90$ km, the intense southward wind fields are formed from May to August, and those result from the mesospheric residual circulation from summer to winter hemispheres. The residual circulation footprint in summer meridional winds is a typical characteristic over northern mid-latitude as observed in Beijing (40.3°N , 116.2°E), Mohe (52.5°N , 122.3°E), and Sorocco (34.1°N , 106.9°W) (Koushik

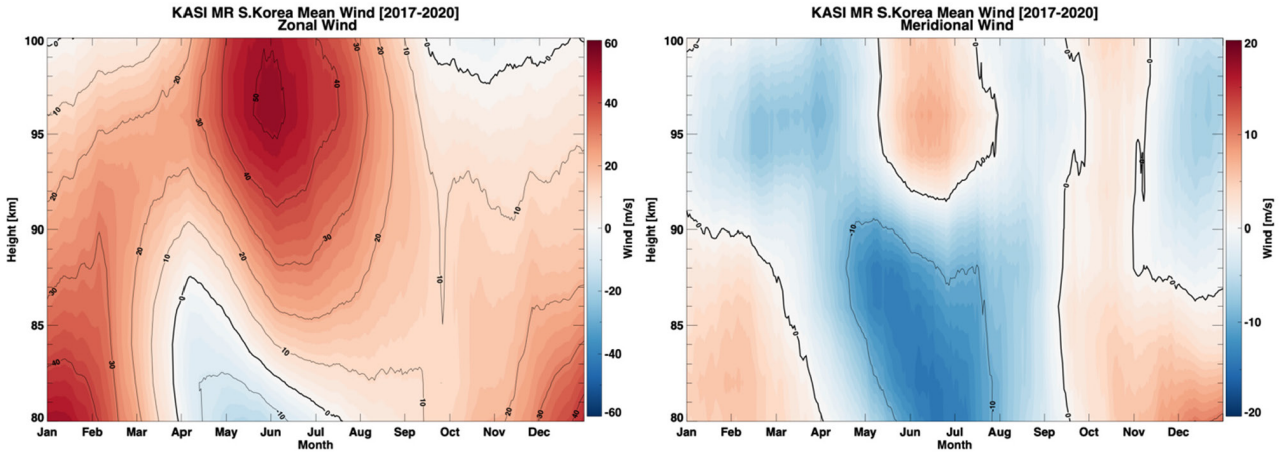


Fig. 3. Mean zonal (top) and meridional (bottom) winds in MLT region over Korean Peninsula obtained from KASI MR for 4-year observation. MLT, mesosphere and lower thermosphere; KASI, Korea Astronomy and Space Science Institute.

et al. 2020; Tang et al. 2021). However, around $z = 92$ km, the meridional wind reverses from southward to northward only over the Korean Peninsula, but not elsewhere. The northward winds can be identified as results of unfiltered northward gravity waves propagating upward through southward wind fields of 90 km or less. At ~ 90 km, this meridional wind reversal can be recognized as a regional characteristic of the Korean Peninsula. Another reason for the formation of northward winds can be attributed to another residual circulation above the mesopause. This additional residual circulation is formed just above the mesopause in the $z = \sim 90\text{--}100$ km domain and is caused by gravity waves propagating in an opposite manner that dissipate or break above the mesopause (Qian & Yue 2017). That is, the primary reversal of zonal winds from westward to eastward at the mesosphere leads to secondary reversal

of zonal winds to westward above the mesopause (Liu 2007; Smith et al. 2011), and the residual circulation also leads to different meridional directions from summer to winter, from winter to summer, in the lower and higher altitude regions, respectively. Therefore, for whatever the potential cause, a meridional reversal above $z = 92$ km over the Korean Peninsula in summer can be formed by gravity waves in the MLT region. Except for the northward wind field in summer, the meridional wind over the Korean Peninsula has typical characteristics of the northern mid-latitude MLT region (Koushik et al. 2020; Tang et al. 2021). Fig. 4 shows Lomb-Scargle periodograms for daily zonal (left) and meridional (right) winds to investigate inter-annual periodic variabilities within a duration of 1-year. Both horizontal winds below $z = 85$ km have strong 1-year periodic change related to monsoons, such as strong westward/southward

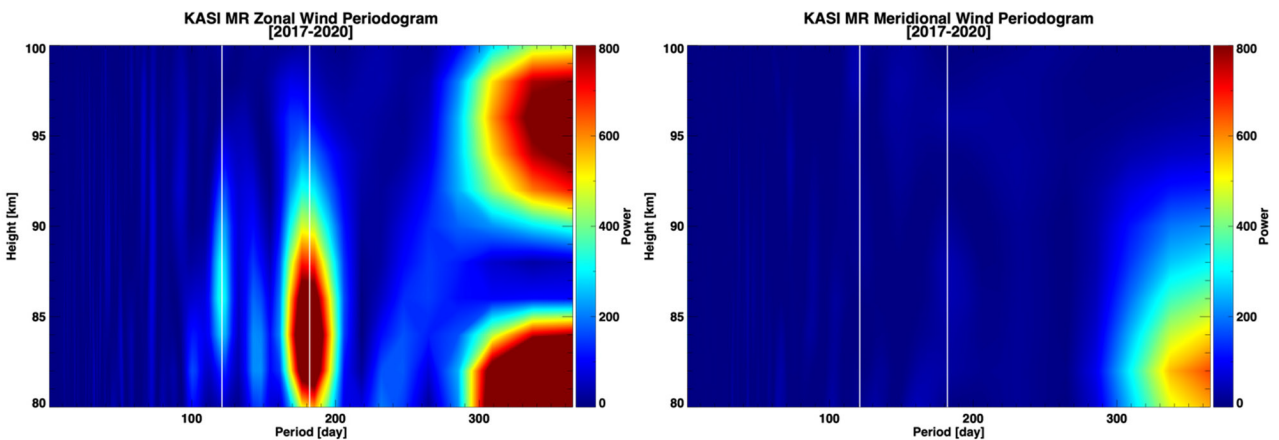


Fig. 4. Lomb-Scargle periodograms for daily zonal (left) and meridional (right) winds in MLT region over Korean Peninsula obtained from KASI MR for 4-year observation. White solid lines indicate periods of 1/3 year (left) and 1/2 year (right), respectively. MLT, mesosphere and lower thermosphere; KASI, Korea Astronomy and Space Science Institute.

winds in summer and eastward/northward winds in winter as shown in Fig. 3. In these regards, the annual variability below $z = 85$ km is due to global mesosphere wind patterns such as strong western jets and residual circulation in summer. Above $z = 90$ km, the annual variation appears only in zonal winds, because the strong eastward wind fields form in summer compared to weaker eastward winds in other seasons. The vertically discontinuous intense power of annual variation in zonal winds indicates a height range of $z = 85$ – 90 km in summer might have large dynamical variabilities such as vertical wind shears and their induced gravity waves (Fritts & Alexander 2003). On the other hand, annual periodic changes do not occur in meridional winds whose magnitudes above $z = 90$ km are weaker than those of below $z = 90$ km in all seasons as seen in Fig. 3. Thus, when capturing spectral power from a periodogram, the magnitude of meridional winds above $z = 90$ km is too small to measure significant periodic variability, even pulse-like events with a time interval. In terms of semi-annual periodicity, the zonal wind SAO is as strong as the annual dynamic force between $z = 80$ – 90 km but does not appear at the meridional winds. Characteristics of SAO can be related to two pulse-type atmospheric characteristics. One is a major pulse as a sign reversal from a strong eastward jet in December to a strong westward jet in June, and the weak zonal wind fields in April and October. These two features have a time interval of about 6 months, and the combination of zonal winds creates an intense SAO feature below $z = 90$ km of the Korean Peninsula. In addition to AO and SAO, ter-annual oscillation (TAO) has significant power in the height range of $z = 85$ – 90 km. The TAO has been rarely reported in previous studies (Krebsbach & Preusse 2007; Shuai et al. 2014; Chen et al. 2019). Chen et al. (2019) revealed that TAOs are difficult to generate in an independent mechanism and are likely to be detected as pulsed occurrences in convective gravity waves in subtropical regions with an active phase of strong consecutiveness for 4 months and a calm phase for the remaining 8 months. Therefore, the detection of TAO through the spectral analysis is also thought to be derived from the pulse-type atmospheric sources with a time interval: strong convective activity such as typhoons in summer or/and gravity waves induced in the MLT region. However, the signal of TAO was not detected in meridional winds, suggesting that further studies are needed.

5. SUMMARY AND CONCLUSIONS

We have investigated hourly, daily, and seasonal cyclical characteristics in zonal and meridional winds in the MLT

region over Korean Peninsula using KASI MR observation for 4-year during 2017–2020. Hourly horizontal winds show that diurnal, and semi-diurnal tides are detected and have a downward phase as upward propagation. Daily variations of winds are presented for seasonal characteristics in terms of altitudes (80–100 km). Below the mesopause in summer, the strong westward winds are regarded as geostrophic winds in the mesosphere due to pressure gradients from the equator to the pole, and the strong southward winds can be caused by the mesospheric residual circulation from the summer hemisphere to the winter hemisphere. Above the mesopause in summer, the strong eastward winds are also typical characteristics such as eastward wave dragging to induce eastward wind fields in the MLT region. In particular, the northward winds above 90 km in summer appears to be a regional characteristics of the entire Korean Peninsular or other residual circulation observed. This might be closely related to gravity waves and their effects. Annual oscillations of horizontal winds are detected in both zonal and meridional winds up to $z = 85$ km, while for above $z = 90$ km they appear only in zonal winds. SAO and TAO are also observed only in zonal winds, and the signatures might be derived from pulse-type atmospheric sources with a time interval. It is the first report for the general environments in the MLT region over the Korean Peninsula. This report might be helpful for any further investigations of the neutral dynamics over the Korean Peninsula using ground-based observation such as airglow all-sky imagers and Fabry-Perot interferometer and etc.

ACKNOWLEDGMENTS

This research was supported by basic research funding from Korea Astronomy and Space Science Institute (KASI) and a National Research Foundation of Korea (NRF) grant funded by the Korea government (MSIT) (2019K2A9A1A0610292012).

ORCID

Hosik Kam	https://orcid.org/0000-0002-3554-0053
Young-Sil Kwak	https://orcid.org/0000-0003-3375-8574
Tae-Yong Yang	https://orcid.org/0000-0002-5725-9828
Yong Ha Kim	https://orcid.org/0000-0003-0200-9423
Jeongheon Kim	https://orcid.org/0000-0003-4953-5228
Jaewook Lee	https://orcid.org/0000-0002-5284-4841
Seonghwan Choi	https://orcid.org/0000-0002-1946-7327
Ji-Hye Baek	https://orcid.org/0000-0002-0230-4417

REFERENCES

- Cevolani G, Tidal activity in the meteor zone over Budrio, Italy, Hand-Book MAP, 25, 121-137 (1987).
- Chen D, Strube C, Ern M, Preusse P, Riese M, Global analysis for periodic variations in gravity wave squared amplitudes and momentum fluxes in the middle atmosphere, *Ann. Geophys.* 37, 487-506 (2019). <https://doi.org/10.5194/angeo-37-487-2019>
- Forbes JM, Vial F, Monthly simulations of the solar semidiurnal tide in the mesosphere and lower thermosphere, *J. Atmos. Sol. Terr. Phys.* 51, 649-661 (1989). [https://doi.org/10.1016/0021-9169\(89\)90063-9](https://doi.org/10.1016/0021-9169(89)90063-9)
- Fritts DC, Alexander MJ, Gravity wave dynamics and effects in the middle atmosphere, *Rev. Geophys.* 41, 1003 (2003). <https://doi.org/10.1029/2001RG000106>
- Garcia RR, Dunkerton TJ, Lieberman RS, Vincent RA, Climatology of the semiannual oscillation of the tropical middle atmosphere, *J. Geophys. Res.* 102, 26019-26032 (1997). <https://doi.org/10.1029/97JD00207>
- Holdsworth DA, Angle of arrival estimation for all-sky interferometric meteor radar systems, *Radio Sci.* 40, RS6010 (2005). <https://doi.org/10.1029/2005RS003245>
- Holdsworth DA, Reid IM, Cervera MA, Buckland Park all-sky interferometric meteor radar, *Radio Sci.* 39, RS5009 (2004). <https://doi.org/10.1029/2003RS003014>
- Holton JR, Wehrbein WM, A numerical model of the zonal mean circulation of the middle atmosphere, *Pure Appl. Geophys.* 118, 284-306 (1980). <https://doi.org/10.1007/BF01586455>
- Kam H, Kim YH, Mitchell NJ, Kim JH, Lee C, Evaluation of estimated mesospheric temperatures from 11-year meteor radar datasets of King Sejong station (62°S, 59°W) and Esrange (68°N, 21°E), *J. Atmos. Sol. Terr. Phys.* 196, 105148 (2019). <https://doi.org/10.1016/j.jastp.2019.105148>
- Koushik N, Kumar KK, Ramkumar G, Subrahmanyam KV, Kumar GK, et al., Planetary waves in the mesosphere lower thermosphere during stratospheric sudden warming: observations using a network of meteor radars from high to equatorial latitudes. *Clim. Dyn.* 54, 4059-4074 (2020). <https://doi.org/10.1007/s00382-020-05214-5>
- Krebsbach M, Preusse P, Spectral analysis of gravity wave activity in SABER temperature data, *Geophys. Res. Lett.* 34, L03814 (2007). <https://doi.org/10.1029/2006GL028040>
- Kwak YS, Yang TY, Kil H, Phanikumar DV, Lee JJ, et al., Characteristics of the E- and F-region field-aligned irregularities in middle latitudes: initial results obtained from the Daejeon 40.8 MHz VHF radar in South Korea, *J. Astron. Space Sci.* 31, 15-23 (2014). <https://doi.org/10.5140/JASS.2014.31.1.15>
- Lieberman RS, Long-term variations of zonal mean winds and (1,1) driving in the equatorial lower thermosphere, *J. Atmos. Sol. Terr. Phys.* 59, 1483-1490 (1997). [https://doi.org/10.1016/S1364-6826\(96\)00150-2](https://doi.org/10.1016/S1364-6826(96)00150-2)
- Lilienthal F, Jacobi, C, Geißler C, Forcing mechanisms of the terdiurnal tide, *Atmos. Chem. Phys.* 18, 15725-15742 (2018) <https://doi.org/10.5194/acp-18-15725-2018>
- Lindzen RS, Turbulence and stress owing to gravity wave and tidal breakdown, *J. Geophys. Res. Oceans.* 86, 9707-9714 (1981). <https://doi.org/10.1029/JC086iC10p09707>
- Lindzen RS, Chapman S, *Atmospheric Tides* (D. Reidel, Dordrecht, 1970).
- Liu HL, On the large wind shear and fast meridional transport above the mesopause, *Geophys. Res. Lett.* 34, L08815 (2007). <https://doi.org/10.1029/2006GL028789>
- Namboothiri SP, Kishore P, Murayama Y, Igarashi K, MF radar observations of terdiurnal tide in the mesosphere and lower thermosphere at Wakkanai (45.4°N, 141.7°E), Japan, *J. Atmos. Sol. Terr. Phys.* 66, 241-250 (2004). <https://doi.org/10.1016/j.jastp.2003.09.010>
- Pancheva D, Mukhtarov P, Smith AK, Climatology of the migrating terdiurnal tide (TW3) in SABER/TIMED temperatures, *J. Geophys. Res. Space Phys.* 118, 1755-1767 (2013). <https://doi.org/10.1002/jgra.50207>
- Qian L, Yue J, Impact of the lower thermospheric winter-to-summer residual circulation on thermospheric composition, *Geophys. Res. Lett.* 44, 3971-3979 (2017) <https://doi.org/10.1002/2017GL073361>
- Shuai J, Zhang SD, Huang CM, Yi F, Huang KM, et al., Climatology of global gravity wave activity and dissipation revealed by SABER/TIMED temperature observations, *Sci. China Technol. Sci.* 57, 998-1009 (2014). <https://doi.org/10.1007/s11431-014-5527-z>
- Smith AK, Structure of the terdiurnal tide at 95 km, *Geophys. Res. Lett.* 27, 177-180 (2000). <https://doi.org/10.1029/1999GL010843>
- Smith AK, Garcia RR, Marsh DR, Richter JH, WACCM simulations of the mean circulation and trace species transport in the winter mesosphere, *J. Geophys. Res.* 116 (2011). <https://doi.org/10.1029/2011JD016083>
- Tang Q, Zhou Y, Du Z, Zhou C, Qiao J, et al., A comparison of meteor radar observation over China region with horizontal wind model (HWM14). *Atmosphere.* 12, 98 (2021). <https://doi.org/10.3390/atmos12010098>
- Thayaparan T, The terdiurnal tide in the mesosphere and lower thermosphere over London, Canada (43°N, 81°W), *J. Geophys. Res.* 102, 21695-21708 (1997). <https://doi.org/10.1029/97JD01839>

- Wu Q, Chen Z, Mitchell N, Fritts D, Iimura H, Mesospheric wind disturbances due to gravity waves near the Antarctica Peninsula, *J. Geophys. Res. Atmos.* 118, 7765-7772 (2013). <https://doi.org/10.1002/jgrd.50577>
- Yang TY, Kwak YS, Kil H, Lee YS, Lee WK, et al., Occurrence climatology of F region field-aligned irregularities in middle latitudes as observed by a 40.8 MHz coherent scatter radar in Daejeon, South Korea, *J. Geophys. Res.* 120, 10107-10115 (2015). <https://doi.org/10.1002/2015JA021885>
- Yang TY, Kwak YS, Lee J, Park J, Choi S, The first report on the afternoon E-region plasma density irregularities in middle latitude, *J. Astron. Space Sci.* 38, 135-143 (2021). <https://doi.org/10.5140/JASS.2021.38.2.135>
- Younger PT, Pancheva D, Middleton HR, Mitchell NJ, The 8-hour tide in the Arctic mesosphere and lower thermosphere, *J. Geophys. Res.* 107, 1420 (2002). <https://doi.org/10.1029/2001JA005086>
- Zhao G, Liu L, Ning B, Wan W, Xiong J, The terdiurnal tide in the mesosphere and lower thermosphere over Wuhan (30°N, 114E), *Earth Planets Space.* 57, 393-398 (2005). <https://doi.org/10.1186/BF03351823>